Pharmacokinetic-directed dosing of vandetanib and docetaxel in a mouse model of human squamous cell carcinoma

Erica L. Bradshaw-Pierce,[1] Courtney A. Steinhauer,[3] David Raben,[2] and Daniel L. Gustafson[2,3,4]

[1]Division of Medical Oncology, School of Medicine, and [2]University of Colorado Cancer Center, University of Colorado Health Sciences Center, Aurora, Colorado and [3]Animal Cancer Center and [4]Department of Clinical Sciences, College of Veterinary Medicine and Biomedical Sciences, Colorado State University, Fort Collins, Colorado

Abstract

Docetaxel, usually administered according to maximum tolerated dose (MTD), can inhibit endothelial cell proliferation at low nanomolar concentrations. Docetaxel may exert antiangiogenic effects if dosed so plasma levels are maintained at low nanomolar concentrations over a prolonged time. We evaluated metronomic and MTD-based dosing of docetaxel with and without vandetanib, a vascular endothelial growth factor receptor-2 and epidermal growth factor receptor tyrosine kinase inhibitor with antiangiogenic and antitumor activity, in a head and neck xenograft model. A murine physiologically based pharmacokinetic model was modified to predict docetaxel distribution following i.p. administration to design dosing regimens that target prespecified plasma concentrations, for antiendothelial effects (metronomic), or exposure, to mimic 30 mg/m^2 (weekly/MTD) docetaxel in humans. Animals were treated for 28 days with 1 mg/kg/d (DTX1) or 6 mg/kg q4d (DTX6) docetaxel with or without vandetanib (15 mg/kg/d p.o.) in mice bearing UMSCC2 tumor xenografts. The DTX1 dosing scheme was adjusted to treatment for 10 days followed by 9 days off due to severe gastrointestinal toxicity. All treatment groups significantly reduced tumor volume, tumor proliferation (Ki-67), and tumor endothelial cell proliferation (Ki-67/von Willebrand factor) compared with control. Addition of vandetanib to docetaxel treatment significantly enhanced tumor growth inhibition over single-agent therapy. A positive correlation of tumor endothelial cell proliferation with tumor growth rates demonstrates vandetanib and docetaxel antiangiogenic effects. Due to the morbidity observed with DTX1 treatment, it is difficult to clearly ascertain if metronomic schedules will be effective for treatment. Docetaxel with vandetanib is effective in treating UMSCC2 xenografts at concentrations relevant to exposures in humans. [Mol Cancer Ther 2008;7(9):3006–17]

Received 4/21/08; revised 6/9/08; accepted 6/25/08.

Grant support: National Cancer Institute/NIH predoctoral fellowship CA99942 (E.L. Bradshaw-Pierce) and National Cancer Institute grant CA101988 (D.L. Gustafson).

The costs of publication of this article were defrayed in part by the payment of page charges. This article must therefore be hereby marked *advertisement* in accordance with 18 U.S.C. Section 1734 solely to indicate this fact.

Requests for reprints: Erica L. Bradshaw-Pierce, Division of Medical Oncology, School of Medicine, University of Colorado Health Sciences Center, 12801 East 17th Avenue, Room L18-8401G, P.O. Box 6511, MS 8117, Aurora, CO 80045. Phone: 303-724-0908; Fax: 303-724-3879. E-mail: Erica.Pierce@uchsc.edu

doi:10.1158/1535-7163.MCT-08-0370

Introduction

Angiogenesis is a process largely regulated by paracrine signaling through growth factors and their binding to receptor tyrosine kinases. As tumors grow in size, cells upregulate the expression of proangiogenic factors to recruit endothelial cells to form a vascular network that will provide oxygen and nutrients to the tumor (1, 2). Vascular endothelial growth factor (VEGF), a key proangiogenic factor, plays a critical role in endothelial cell survival, proliferation, migration, and capillary tube formation (3, 4). The importance of VEGF signaling, through activation of VEGF receptor-2, in pathogenic angiogenesis has been recognized and has led to the recent development of compounds designed to inhibit this and other receptor-mediated signal transduction pathways important in tumor progression such as epidermal growth factor receptor (EGFR) signaling. EGFR and its ligands, EGF and transforming growth factor-α, are overexpressed in several different tumor types (5) and EGFR can be found on tumor-associated endothelial cells (6, 7). Activation of EGFR leads to downstream signaling of pathways that are critical regulators of tumor growth, invasion, angiogenesis, and metastasis (8, 9).

Vandetanib (Zactima/ZD6474, AstraZeneca), a 4-anilinoquinazoline, is an orally available synthetic small molecule designed to bind to the intracellular kinase domain of receptor tyrosine kinases, preventing phosphorylation and disrupting the necessary signal transduction for cell proliferation (10, 11). Vandetanib has shown potent, selective activity against VEGF receptor-2 and has activity against EGFR (10, 11). The dual activity of vandetanib allows a single molecularly targeted agent to inhibit two key pathways in tumor growth by targeting the tumor vasculature and the tumor cell population. Preclinical models have shown the utility of vandetanib as a single agent in numerous tumor models (12) as well as its ability to enhance the activity of cytotoxic chemotherapy (13) and radiation therapy (14, 15).

A recent clinical study reported that the addition of vandetanib to docetaxel therapy in patients with

stage III/IV non-small cell lung cancer led to a significant increase in progression-free survival versus docetaxel alone (16). Docetaxel, a semisynthetic taxane that exerts its effects by promoting microtubule assembly and inhibiting their depolymerization, is an important chemotherapeutic agent currently approved for use for the treatment of breast, prostate, and non-small cell lung cancer and has demonstrated activity against ovarian, bladder, and head and neck cancers (17–21). Docetaxel use in head and neck squamous cell carcinoma (HNSCC) is often combined with radiation therapy and the dose and schedule of docetaxel are modified due to excessive nonhematologic (grade III/IV mucositis) toxicity (22, 23). The incorporation of anti-EGFR therapies in HNSCC has been effective with added efficacy and no increase in toxicity when combined with radiation therapy (14, 15, 24, 25). The ability of vandetanib to enhance docetaxel effects (13, 16) have positive interactions with radiation therapy (14, 15), and the lack of increased toxicity with anti-EGFR/radiation therapy combinations gives potential for this agent to be beneficial in HNSCC. An important question to be addressed is the optimization of docetaxel schedules with vandetanib and whether metronomic schedules can be considered. Docetaxel has shown antiangiogenic activity in preclinical studies (26–28) and the potential for enhanced activity due to VEGF receptor-2 inhibition by vandetanib warrants investigation of schedules optimized for antiendothelial activity.

Docetaxel exhibits a complex pharmacologic profile with high interpatient variability in pharmacokinetics (29), making the use of pharmacokinetic models that can predict concentrations *in vivo* under various dosing schema attractive. Physiologically based pharmacokinetic (PBPK) models can aid in the development of optimized clinical protocols that incorporate chemotherapeutics, molecularly targeted agents, and combination of the two. PBPK models use biochemical, physiologic, and chemical engineering principles to mathematically describe blood and tissue distribution of compounds. One of the greatest strengths of PBPK models, compared with classic compartmental or noncompartmental pharmacokinetic modeling, is the ability to predict *a priori* drug distribution and to extrapolate between doses, routes of administration, and species (30).

One of the shortcomings of preclinical studies is the use of doses in mice that are not achievable in humans. Ideally, dose levels and schedules used in preclinical studies should simulate exposures observed in human patient populations. This may increase the potential of preclinical animal models to better predict the efficacy of treatment modalities, combinations, and schedules in humans. In the study presented here, we conducted an *in vivo* preclinical study of vandetanib, docetaxel, and combinations of the two in a mouse xenograft model of HNSCC using dose levels and schedules derived using PBPK model simulations for docetaxel (31) and empirically determined steady-state pharmacokinetics of vandetanib (32) to target prespecified plasma concentrations based on human drug exposure scenarios and putative antiendothelial drug levels. We compared antiendothelial schedules, where drug levels targeted were based on *in vitro* endothelial cell response to docetaxel and vandetanib, to maximum tolerated dose (MTD)-based schedules of docetaxel.

Materials and Methods

Chemicals and Reagents

Docetaxel (Taxotere; Sanofi-Aventis) for *in vitro* studies was purchased from LKT Labs, and docetaxel for *in vivo* studies was obtained from the University of Colorado Hospital Pharmacy and as a gift from Sanofi-Aventis. Vandetanib (ZD6474; Zactima) was a generous gift from AstraZeneca. Docetaxel and vandetanib stock solutions for *in vitro* experiments were made in DMSO (Fisher Scientific). All other materials used were purchased from either Fisher Scientific or Sigma unless specified.

Cells and Culture Conditions

Head and neck tumor cells, UMSCC2 (University of Michigan), were maintained on tissue culture plates (BD Falcon) in DMEM (Cellgro) supplemented with 10% heat-inactivated fetal bovine serum (Cellgro) and penicillin (100 units/mL)-streptomycin (100 μg/mL; Life Technologies). Primary endothelial cells were grown on 2% gelatin-coated tissue culture plates in DMEM (BioWhittaker) supplemented with 2 mmol/L L-glutamine (Life Technologies), 1 mmol/L sodium pyruvate (Life Technologies), 1% nonessential amino acids (Life Technologies), 50 mmol/L 2-mercaptoethanol (Life Technologies), 20 mmol/L HEPES (Life Technologies), penicillin (100 units/mL)-streptomycin (100 μg/mL; Life Technologies), 12 units/mL heparin, 20% heat-inactivated fetal bovine serum (Life Technologies), and 100 μg/mL endothelial cell growth supplement (BD Biosciences). MCF-7 cells (American Type Culture Collection) were maintained on tissue culture plates in RPMI supplemented with 10% heat-inactivated fetal bovine serum with penicillin/streptomycin and 0.0015 units/mL insulin (Humulin R; Eli Lilly). All cells were maintained at 37°C in a humidified incubator with 5% CO_2. All *in vitro* drug treatments were conducted with the use of complete growth medium.

Animals

Female BALB/c mice (retired breeders) were purchased from Charles River Laboratories and 5- to 10-week -old female athymic nude mice were purchased from the National Cancer Institute. Animals were housed (3-5 per cage) in polycarbonate cages and kept on a 12 h light/dark cycle. Food and water were given *ad libitum*. All studies were conducted in accordance with the NIH Guidelines for the Care and Use of Laboratory Animals, and animals were housed in a facility accredited by the American Association for Accreditation of Laboratory Animal Care.

Isolation of Primary Endothelial Cells from Mouse Lung

Primary endothelial cells were isolated from the lungs of female BALB/c mice by immunomagnetic bead separation. The method used is a slightly modified procedure from Marelli-Berg et al. (33). Briefly, mice were anesthetized with isoflurane and sacrificed by cardiac stick exsanguination.

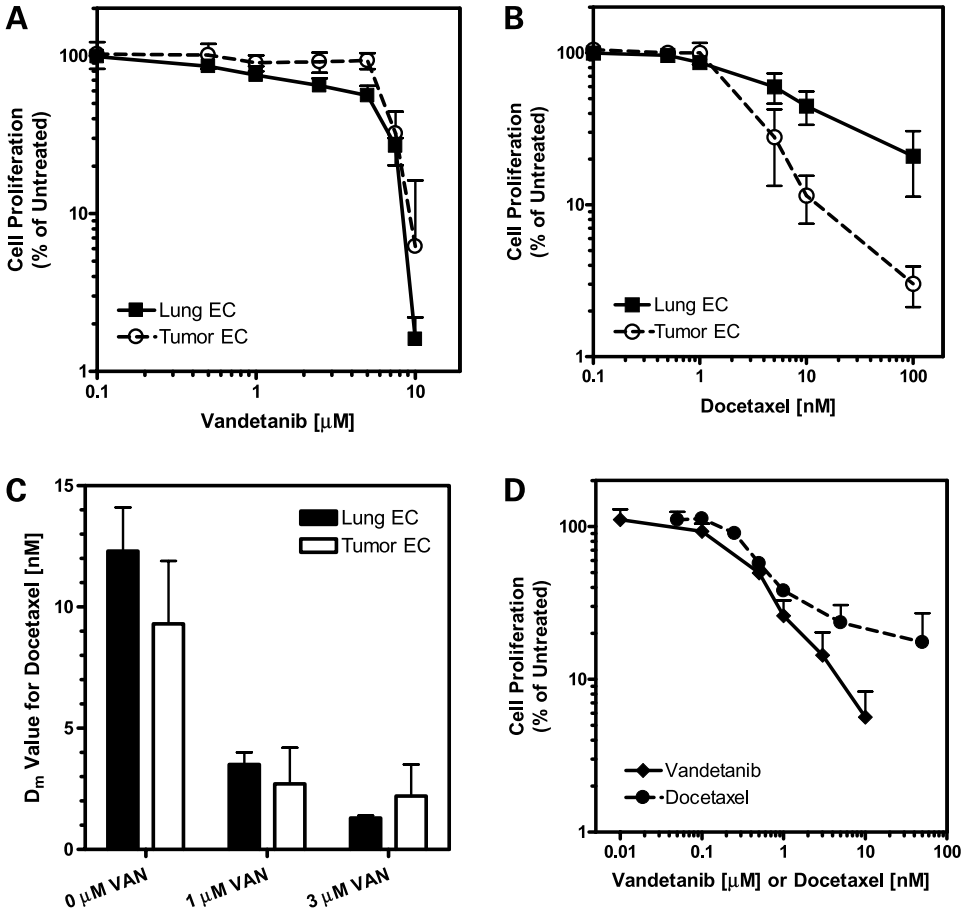

Figure 1. Effect of vandetanib (**A**), docetaxel (**B**), and vandetanib with docetaxel (**C**) on primary lung (*black symbols/bars*) and primary tumor (*open symbols/bars*) endothelial cells. The effects of vandetanib (♦) and docetaxel (●) were also evaluated in UMSCC2 head and neck carcinoma cells (**D**). Cells were exposed continuously for 120 h before MTT assay. Mean ± SD of a minimum of three experiments.

Mouse lung was excised, minced, rinsed in cold PBS, and digested by type II collagenase (Worthington Biochemical) and collagenase A (Roche) at 37°C for 1 h. The digest was then passed through a 50 μm cell strainer (BD Bioscience) to remove undigested tissue. Cells were subsequently washed with PBS with 1% FCS (Life Technologies), counted, and incubated in 10% mouse serum for 30 min at 4°C. Following a wash step, cells were incubated with rat anti-CD31, rat anti-CD105 (BD PharMingen), and biotinylated isolectin B4 (Vector Laboratories) for 30 minutes at 4°C. Cells were washed then incubated with anti-rat and streptavidin-conjugated magnetic microbeads (Miltenyi Biotec) for 30 min at 4°C. Magnetically labeled cells were then separated on a Vario Macs magnetic column (Miltenyi Biotec). Cells were seeded on 2% gelatin (Sigma)-coated tissue culture plates (BD Falcon) and cultured as described earlier. Cells were kept for up to 10 passages.

Isolation of Primary Endothelial Cells from MCF-7 Tumor Xenografts

Endothelial cells from MCF-7 tumor xenografts were isolated similar to the method described by St.Croix et al. (34) and similar to the method used to isolate lung endothelial cells as described above. Tumors were resected, minced, rinsed in cold PBS, and digested by type II collagenase, collagenase A, and elastase (Roche) with DNase I (Roche) at 37°C for 1 h with gentle shaking. Following filtration through a 50 μm cell strainer, cells were separated through a 30% Percoll gradient (Sigma). The remainder of the isolation was done as described above for the mouse lung endothelial cells.

Cell Proliferation Assay

Growth-inhibitory effects of vandetanib and docetaxel were determined by MTT assay. Cells were plated in 96-well plates (BD Falcon) at a density of 1,000 to 2,000 per well and incubated overnight prior to treatment. Drug solutions were made up in appropriate growth media and all stock solutions were diluted at least 1:100. Cells were treated with drug-containing media continuously for 120 h followed immediately by the MTT assay. Fifty micrograms of MTT per well was added to cells in serum-free DMEM. Cells were incubated at 37°C with 5% CO_2 for 4 h. Media was removed and replaced with 100 μL DMSO. Plates were read on a plate reader (Molecular Devices) at 550 nm with Softmax version 2.32. The assay was repeated a minimum of three times for each drug.

MCF-7 Xenografts

Animals were implanted with slow-release Silastic 17β-estradiol pellets (35) s.c. between the shoulders, at least 24 h before MCF-7 tumor cell inoculation. MCF-7 cells were harvested and resuspended in a 1:1 mixture of

serum-free RPMI 1640 and Matrigel (BD Bioscience). Five million cells per mouse were injected s.c. into the rear flank.

UMSCC2 Xenograft Studies

UMSCC2 cells were harvested and resuspended in a 1:1 mixture of serum-free DMEM and Matrigel. Two million cells per mouse were injected s.c. into the rear flank. Tumors volumes, measured by digital calipers, were calculated by V (mm^3) = length $\times$ (width)^2 $\times$ 0.5236. When tumors reached an average volume of 125 mm^3, mice were randomized into groups (9-10 mice per group) and treatment began on day 1 and continued for 28 days. Animals received either vehicles, 15 mg/kg vandetanib alone, 1 mg/kg docetaxel (DTX1) alone, 6 mg/kg docetaxel (DTX6) alone, or a combination of vandetanib and DTX1 or vandetanib and DTX6. Docetaxel doses administered were determined by murine PBPK model simulations that approximated a MTD dose observed in humans (DTX6) or targeted trough plasma concentrations greater than 1 nmol/L on daily administration (DTX1). Mice received vandetanib resuspended in 1% Tween 80 by oral gavage daily for 28 days. Docetaxel was prepared and diluted in 0.9% sodium chloride. Mice receiving 6 mg/kg docetaxel were treated every 4 days for 28 days (8 total treatments) by i.p. injection. Mice receiving 1 mg/kg docetaxel were treated i.p. for 10 consecutive days, had a 9-day recovery period, and then received treatment again for the remaining 9 days. For combination treatment, mice were administered vandetanib immediately followed by docetaxel injection. Tumor measurements were made every other day during treatment (days 1-28) and twice weekly post-treatment (days 29-54). Animals that experienced treatment-related toxicity were placed on s.c. saline and NutriCal support. Animals were sacrificed when they were moribund. On day 10 of treatment, 3 animals per group were sacrificed, approximately 2 hours post-treatment, and tumors were excised and formalin-fixed for immunohistochemical analysis.

Immunohistochemical Staining for Active Caspase-3, Ki-67, and von Willebrand Factor

Immunohistochemical staining was done on formalin-fixed and paraffin-embedded tumor sections collected on day 10 of the study. Tissue sections (4 μm thick; on positively charged slides) were deparaffinized in xylene with subsequent rehydration. Heat-induced epitope retrieval was done by incubating the slides at 125°C for 1 min in an EDTA-based solution (DAKOCytomation) at pH 9.0 (active caspase-3) or pH 6.0 [for Ki-67 and von Willebrand factor (vWF)]. Active caspase-3 was visualized using active caspase-3 rabbit anti-human/mouse (1:1,000 dilution overnight at 4°C; R&D Systems) followed with Texas red anti-rabbit IgG (1:100 dilution; 1 h at 4°C; Vector Laboratories). For the dual stain of Ki-67 and vWF, sections were stained sequentially. Ki-67 rat anti-mouse monoclonal antibody (1:25 dilution; overnight at 4°C; DAKOCytomation) was applied followed by the secondary antibody, fluorescein anti-rat IgG (1:100 dilution; 1 h at 4°C; Vector Laboratories). Next, a polyclonal rabbit vWF was applied (1:100 dilution; 1 h at room temperature; DAKOCytomation) pursued with Texas red anti-rabbit IgG secondary antibody (1:100 dilution; 1 h at 4°C). Slides were mounted using Vecta Shield with 4,6-diamidine-2-phenylindole (Vector Laboratories). For each slide, five still images (at each wavelength) were acquired using an Axioplan 2 imaging universal microscope with the necessary fluorescent wavelengths to visualize fluorescein (excision 495 nm, emission 515 nm), Texas red (excision 595 nm, emission 615 nm), and 4,6-diamidine-2-phenylindole (excision 360 nm, emission 460 nm). Images were analyzed using AxioVision to count the positive fluorescent pixels per image section, ensuring at least a 95% capture rate. For determination of epithelial proliferation, single images visualizing fluorescein (Ki-67) and Texas red (vWF) were overlaid and resulting double-positive cells (yellow) counted.

Docetaxel i.p. PBPK Model Development

A PBPK model for docetaxel plasma and tissue distribution in mice was developed previously in our laboratory (31). This model describes docetaxel distribution following a single i.v. dose. We modified this PBPK model to describe docetaxel distribution following a single i.p. bolus dose and repeated i.p. dosing. All parameters, listed in Supplementary Tables S1 and S2, used for the i.v. docetaxel PBPK model remained the same as reported previously (31). A schematic representation of the model used here is shown in Supplementary Fig. S1. Additional details of the development of the i.p. docetaxel PBPK model are described in Supplementary Material.

Determination of Median Lethal Dose Values for *In vitro* Experiments

A general equation used to describe dose-response relationship was derived by Chou (36, 37) as:

$$\frac{f_a}{f_u} = \left(\frac{D}{D_m}\right)^m \quad (1)$$

where f_a is the fraction affected by the dose, f_u is the fraction unaffected ($f_u = 1 - f_a$), D is the dose of drug, D_m is the median-effect dose, and m is an exponent signifying the sigmoidicity (shape) of the dose-effect curve. A median-effect plot, plot of x = log (D) versus y = log (f_a / f_u), described in Eq. (2.2), is the logarithmic form of Eq. (2.1).

$$\log\left(\frac{f_a}{f_u}\right) = m\log(D) - m\log(D_m) \quad (2)$$

Using the slope and intercept obtained from the median-effect plot, the median lethal dose can be determined by

$$D_m = 10^{-(y-\text{intercept})/m} \quad (3)$$

Tumor Growth Rate Calculations and Statistical Analysis

Tumor growth rates were calculated by liner regression of the tumor volume versus time plots for individual tumors for the periods of 1 to 14 and 15 to 28 days. The Student's t test was used to determine statistical significance between two groups when data was normally

distributed and one-way ANOVA analyses with a Tukey post-test was used for the comparison of multiple groups. Analysis was performed with Prism version 4.02. P values < 0.05 were considered statistically significant.

Results

In vitro Antiproliferative Activity of Vandetanib and Docetaxel

We first investigated the antiproliferative activity of vandetanib and docetaxel in murine primary endothelial cells. Endothelial cells were isolated from mouse lung and human tumor xenografts grown in the flanks of mice. We verified the selection of endothelial cells by detection of surface receptors VEGF receptor-2, CD105, and CD106 (data not shown). Cells were exposed to vandetanib or docetaxel in normal growth medium for 120 h. This prolonged exposure time was chosen since vandetanib is administered as a once daily dose and steady-state levels should be maintained and since we were interested in investigating the use of more frequent, protracted schedules of docetaxel for antiangiogenic therapy. Lung and tumor endothelial cells responded similarly to vandetanib with median lethal dose values (D_m) of 3.8 ± 1.1 and 6.1 ± 1.5 μmol/L, respectively (Fig. 1A). Although these values appear to be high and are in fact higher than previously reported IC_{50} values of vandetanib in HUVEC cells (10), our treatments took place in complete medium conditions (20% fetal bovine serum + ECGS) and not under direct and exclusive stimulation of VEGF. At low concentrations (<10 nmol/L), tumor and lung endothelial cell lines responded similarly with D_m values of 9.3 ± 2.6 and 12.3 ± 1.8 nmol/L, respectively (Fig. 1B).

Due to the potential for additive and synergistic benefit of administering molecularly targeted agents in combination with cytotoxic agents, we investigated how vandetanib affected endothelial cell response to docetaxel (Fig. 1C). The addition of vandetanib to docetaxel provided an additive to synergistic benefit with CI values ranging from 0.99 for tumor endothelial cells treated with 3 μmol/L vandetanib and docetaxel to 0.47 for lung endothelial cells treated with 1 μmol/L vandetanib and docetaxel.

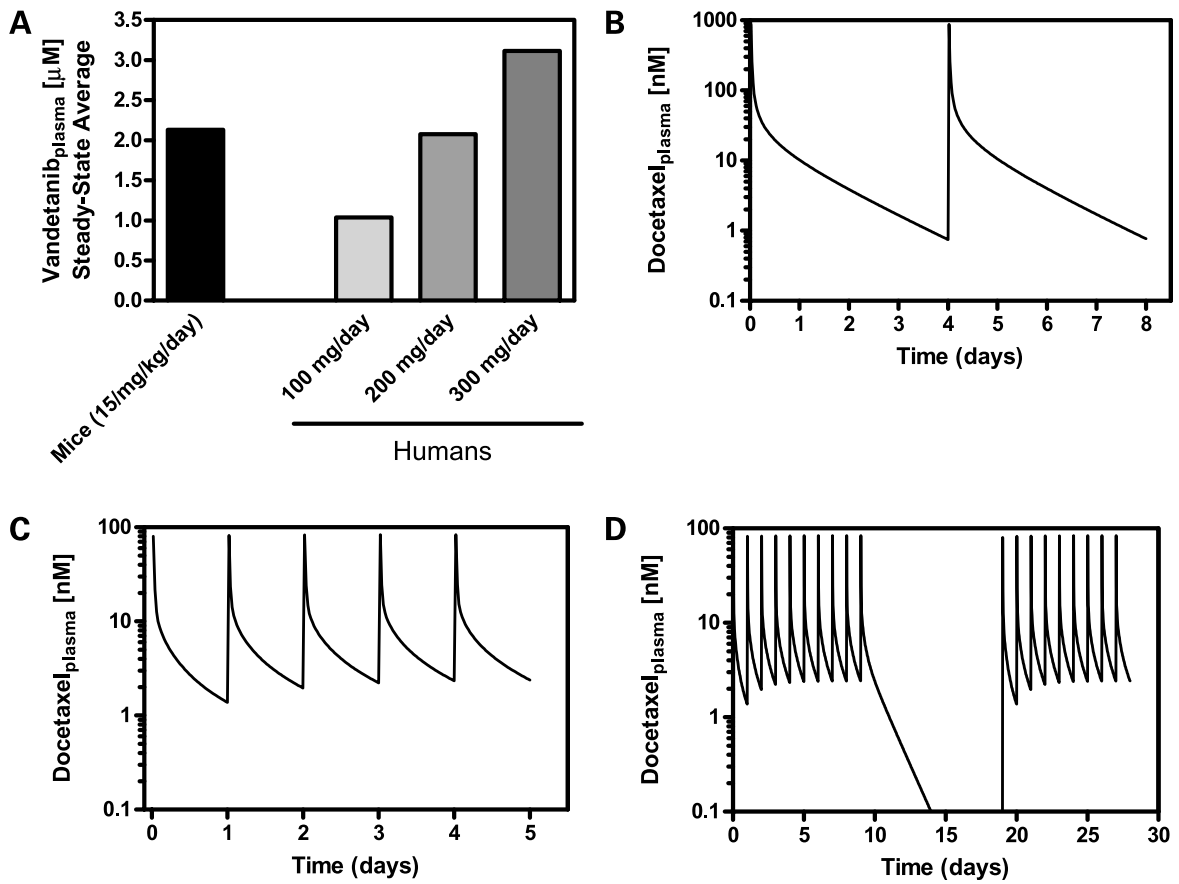

Figure 2. **A,** average steady-state plasma levels of vandetanib in mice and humans. **B,** PBPK model simulation showing docetaxel plasma concentrations following a MTD-based dosing schedule in mice. Simulations were generated based on a 6 mg/kg dose administered i.p. every 4 d. **C,** PBPK model simulation showing docetaxel plasma concentrations following a metronomic dosing schedule in mice. Simulations were generated based on a daily i.p. dose of 1 mg/kg. **D,** PBPK model simulation of the 1 mg/kg daily dose modified to account for a 9-d break following the first 10 d of treatment. This break period was included due to unexpected toxicity observed in animals treated with the metronomic schedule of docetaxel.

Table 1. Comparison of pharmacokinetic variables for single-dose and multiple-dose docetaxel in mice and humans

	$t_{1/2}$ (h)	$AUC_{0\rightarrow24}$ (μmol/L h)	C_{max} (nmol/L)	C_{min} (nmol/L)	Total dose delivered (nmol)
Single-dose pharmacokinetics					
Human 30 mg/m²*	27.5 ± 5.5	1.02 ± 0.39	1342 ± 655		63.6 ± 9.6 μmol
Mouse 6 mg/kg i.p.†	11.5	1.23	870		139
Mouse 1 mg/kg i.p.†	11.0	0.14	80		23
Multiple-dose pharmacokinetics					
Mouse 6 mg/kg q4d		12.5‡	876	0.8	975
Mouse 1 mg/kg qd		5.9‡	84	1.4	650
Mouse 1 mg/kg (modified schedule)		3.9‡	84	0	441

* Human plasma pharmacokinetic variables were calculated using a three-compartment models with i.v. infusion input of drug. Data from ref. 31.
† Mouse single-dose plasma pharmacokinetic variables were calculated using noncompartmental analysis of simulated data.
‡ AUC for multiple doses calculated in Microsoft Excel using trapezoidal rule.

The antiproliferative effects of vandetanib and docetaxel were also evaluated in an EGFR-positive HNSCC cell line, UMSCC2 (Fig. 1D). UMSCC2 cells exhibited sensitivity to both vandetanib and docetaxel with D_m values of 0.42 ± 0.07 μmol/L and 0.74 ± 0.10 nmol/L, respectively.

Pharmacokinetic-Directed Dosing of Vandetanib

In a previous study, we used data from human clinical trials with vandetanib and data we gathered from mice and calculated daily dosing that reflected human pharmacokinetic parameters (32). Our calculations show that mice should receive daily dosing of 17.4, 48.6, and 17.8 mg/kg to simulate C_{max}, C_{min}, and AUC levels achieved in humans at 300 mg/d, respectively. Based on this result, we decided to use a daily p.o. dose of 15 mg/kg vandetanib, which should reasonably represent 100 to 300 mg/d vandetanib in humans, doses achieved in the clinic. Figure 2A shows predicted average steady-state vandetanib plasma concentrations in mice at 15 mg/kg/d and in humans.

Docetaxel PBPK Model Simulations for the Development of Pharmacokinetic-Directed Dosing Protocols

Our previously published docetaxel PBPK model (31) was developed to design pharmacokinetic-directed dosing protocols to be tested *in vivo*, the objective of the studies described here. We were interested in investigating the effects of low-dose metronomic schedules of docetaxel on *in vivo* tumor growth/regression and tumor growth rates. Since repeated, frequent (>2 times per week) i.v. injections in a nude mouse are technically very difficult, we decided to administer docetaxel by i.p. injections. This required a modification to the mouse PBPK model to account for the different route of administration and for repeated dosing. The route-modified model was validated (see Supplementary Material for further detail) and then used to determine the amount and schedule to be used that would achieve docetaxel plasma levels and exposures that were clinically relevant. We developed a schedule to be administered to mice that achieved roughly the same AUC seen in a 30 mg/m² dose in humans administered on a weekly schedule. A single dose of 6 mg/kg delivered i.p. to mice achieved an AUC of 1.2 μmol/L h compared with an AUC of approximately 1.0 μmol/L h seen in humans (Table 1). The terminal half-life at 30 mg/m² in humans was about two times longer than the terminal half-life at 6 mg/kg in mice. Therefore, to roughly match a weekly regimen of docetaxel in humans, the 6 mg/kg dose was delivered every 4 days. The resulting model simulation is shown in Fig. 2B. Model simulations were generated using a dosing interval of 96 h for 28 days (duration of the study).

To investigate the use of a metronomic or antiangiogenic schedule with docetaxel, we determined a dose and frequency that would maintain low plasma levels of docetaxel (>1 nmol/L). A single i.p. dose of 1 mg/kg docetaxel results in approximately 10% of the exposure seen at the 6 mg/kg dose in mice or the 30 mg/m² dose in humans (Table 1). The C_{max} at this dose is 80 nmol/L, which drops off to below 25 nmol/L by 1 h post-administration. Based on simulations, to maintain a C_{min} above 1 nmol/L, a 1 mg/kg dose of docetaxel needs to be administered daily. The resulting model simulation of 1 mg/kg delivered i.p. in mice daily is shown in Fig. 2C. Model simulations were generated using a dosing interval of 24 h for 28 days (duration of the study). Table 1 shows comparative pharmacokinetic parameters for docetaxel in humans at 30 mg/m² and in mice at single doses of 6 and 1 mg/kg. We also calculated the total exposure, C_{max}, C_{min}, and total dose delivered (based on a 25 g mouse) based on model simulations for schedules developed for *in vivo* testing: 6 mg/kg q4d and 1 mg/kg qd for 28 days.

Approximately 7 days into the *in vivo* therapeutic study intestinal toxicity was observed in the animals being treated with 1 mg/kg docetaxel. Due to this unexpected toxicity, the 1 mg/kg treatment did not continue for the duration of the experiment. Instead, mice to be treated with 1 mg/kg docetaxel were given a 9-day break period. On day 20 of the study, mice resumed treatment with 1 mg/kg docetaxel i.p. Figure 2D shows the PBPK model simulation reflecting the change in the treatment schedule. Table 1 also reflects the changes to the pharmacokinetic parameters. By day 14, plasma docetaxel levels were negligible. This break period resulted in a reduction of about 34% in the total exposure.

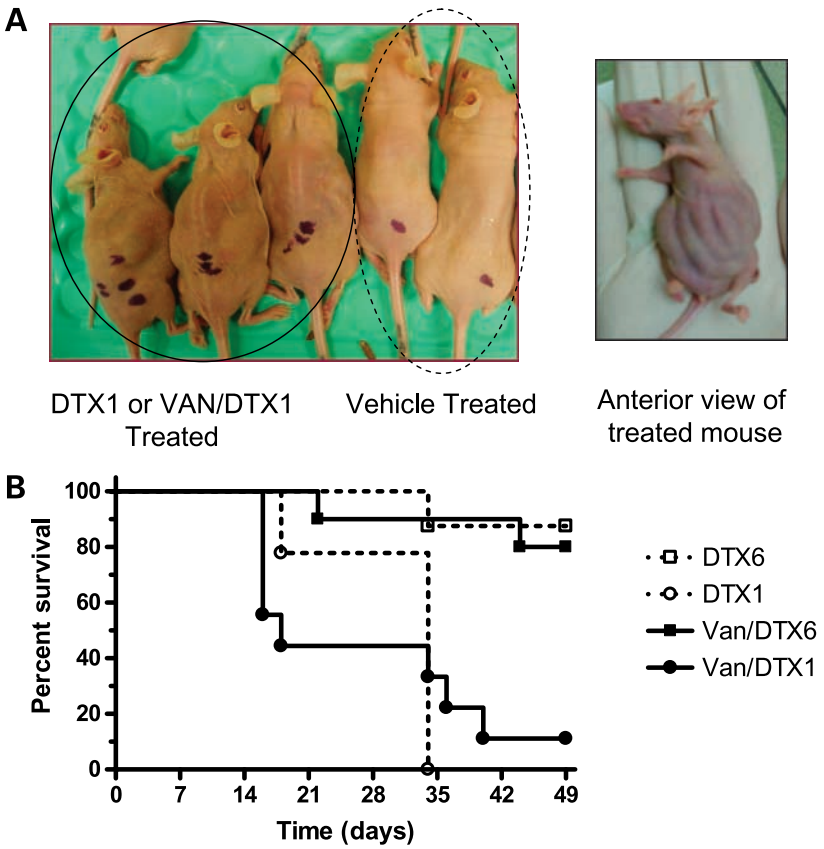

Figure 3. Intraperitoneal metronomic dosing of docetaxel resulted in severe gastrointestinal toxicity in nude mice. **A,** pictures of mice on day 9 of DTX1 or vandetanib/DTX1 treatment compared with vehicle control treated mice. **B,** survival curves of all docetaxel-treated mice. Animals treated with DTX1 alone or with vandetanib experienced significantly more mortality than DTX6 or vandetanib/DTX6-treated mice.

UMSCC2 Tumor Xenograft Response to Vandetanib, Docetaxel, and Combination Therapy

Docetaxel was delivered by i.p. injection at either 6 mg/kg every 4 days (DTX6) for 28 days or 1 mg/kg/d for 10 days followed by a 9-day break period and then daily for 9 days (DTX1). Vandetanib was administered by oral gavage at a dose of 15 mg/kg/d for 28 days. The study was initially designed to have 1 mg/kg docetaxel delivered daily for the entire study; however, severe intestinal toxicity was observed by 10 days (Fig. 3A). In the sick mice, the intestines were visually distended, and on necropsy, the entire length of the intestine was found to be full, indicating a problem with absorption and motility. Some intestinal toxicity was also observed in the 6 mg/kg docetaxel groups; however, it was not as pronounced as the 1 mg/kg groups, so treatment remained as scheduled. Figure 3B shows the survival curves of the different docetaxel treatment groups. No animals from the control or vandetanib treated groups died during the study. Seventeen of 18 animals treated with DTX1 died, whereas only 3 of 18 animals treated with DTX6 died.

The efficacy of vandetanib, docetaxel, and combinations of the two was determined in UMSCC2 tumor xenografts. Figure 4A shows the tumor growth curves for the 28 days of treatment and for 28 days following the conclusion of treatment. Tumors were monitored following treatment to assess tumor regrowth patterns. Fig. 4A (*inset*) shows tumor growth for only the 28-day treatment period. All treatment groups significantly reduced tumor volume compared with control ($P < 0.05$). For the 28-day treatment period, the addition of vandetanib to DTX1 and DTX6 treatment resulted in significantly reduced tumor growth compared with DTX1 or DTX6 single-agent treatment.

Tumor growth rates for individual tumors were calculated for various treatment intervals, days 1 to 14 and 15 to 28 (Fig. 4B). Although tumor measurements were made for 4 weeks post-treatment, growth rates were not calculated for this time frame due to the high mortality rates and resulting lack of sufficient data for some groups. Although none of the groups has significantly different growth rates, the trend indicates a reduction in tumor growth rates for all treatment groups for days 1 to 14. For days 15 to 28, tumor growth rates appeared to be slower for all treatment groups, except for DTX1. It is also worth noting that the vandetanib + DTX6 group had a negative growth rate for the first 14 days of the study indicating tumor regression.

Tumor doubling time was also calculated and is shown in Fig. 4C. Vandetanib, DTX6, and vandetanib + DTX6 groups all had animals with tumors that did not double in volume up to 28 days post-treatment.

Additionally, complete responses, no palpable tumor remaining and no regrowth up to 28 days post treatment, were observed in the vandetanib, DTX6, and vandetanib + DTX6 groups (n = 1, 2, and 1, respectively).

Immunohistochemical Analysis of UMSCC2 Tumors

To investigate the antiproliferative effects of treatment on tumors, on day 10, 3 animals per group were sacrificed approximately 2 h post-treatment and tumor sections collected for immunohistochemical analysis of apoptosis (active caspase-3) and proliferation (Ki-67) by caspase-3 and Ki-67. The largest increase in caspase-3, compared with control, was found in the vandetanib and vandetanib + DTX6 groups (Fig. 5A and C) and all treatment groups showed a significant ($P < 0.05$) decrease in Ki-67 staining (Fig. 5B and C).

Since we were investigating the use of antiangiogenic schedules of docetaxel and since vandetanib also inhibits VEGF receptor-2 in addition to EGFR, we wanted to investigate the effects of treatment on tumor endothelium. Tumor sections were stained with vWF and vessels counted to assess the microvessel density (MVD). Only the DTX6 and vandetanib + DTX6 treatment groups appeared to affect microvessel density (Fig. 5C). However, Ki-67 staining colocalized with vWF showed a significant ($P < 0.001$) decrease in endothelial cell proliferation in all treatment groups (Fig. 5C). Additionally, analysis of tumor growth rate (Fig. 4B) with immunohistochemical indices showed that only proliferation within endothelial cells (dual vWF and Ki-67) showed a positive correlation ($P < 0.05$), whereas neither active caspase-3 nor Ki-67 alone correlated. Although these results

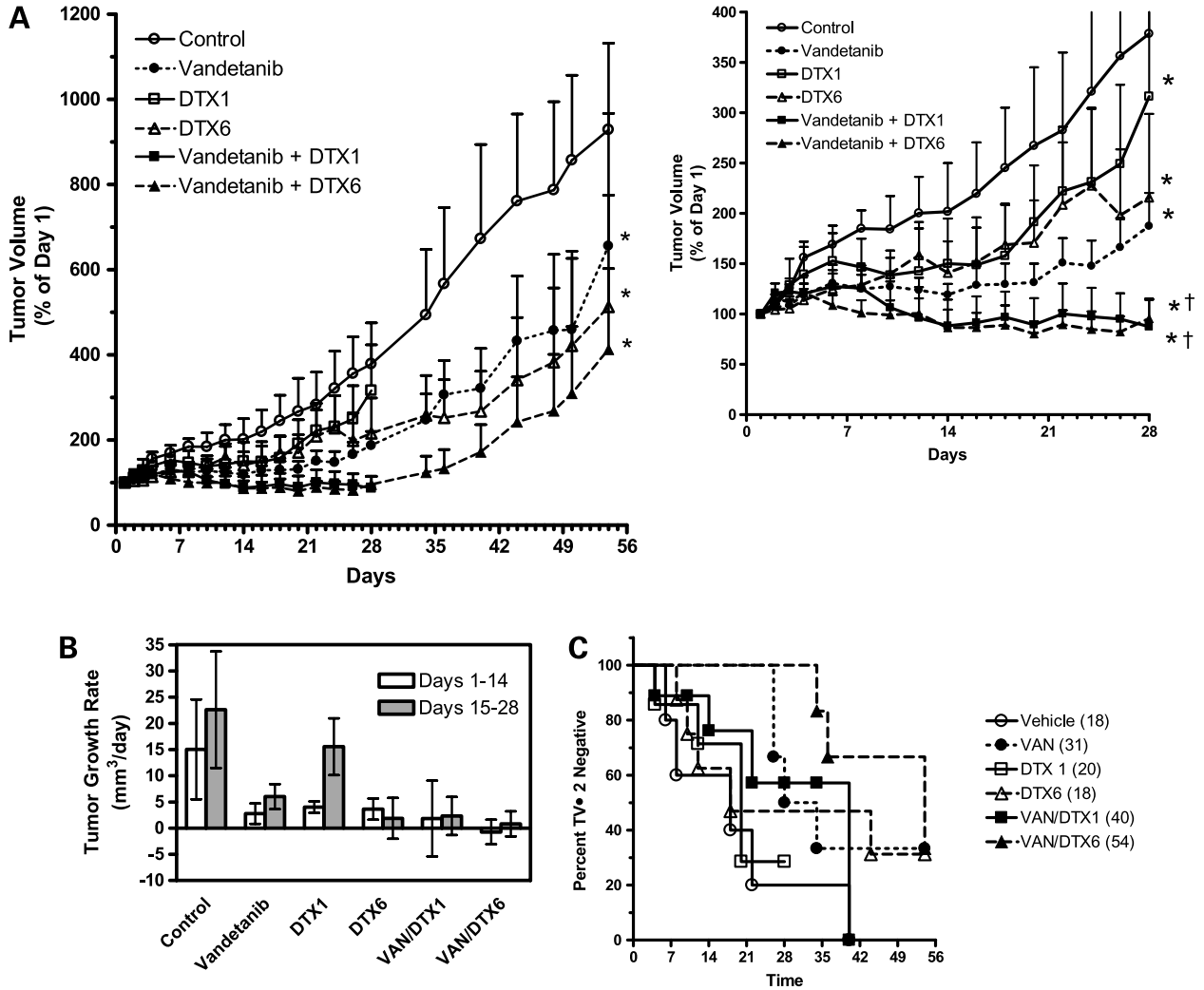

Figure 4. **A,** tumor growth profiles of mice bearing UMSCC2 tumor xenografts treated with vandetanib, docetaxel, and combination of the two. Treatment began on day 1 and continued for 28 days (*inset*). Following treatment, tumor volumes were measured in surviving mice to determine regrowth characteristics. Mean ± SE. *, $P < 0.05$, versus control; †, $P < 0.05$, versus DTX1 or DTX6 treatment alone. **B,** tumor growth rates were calculated for days 1 to 14 and 15 to 28 of treatment for all mice that survived through day 28. Rates were calculated by linear regression of tumor size data for individual tumors. Mean ± SD. **C,** percentage of UMSCC2 tumors that have not doubled from their initial starting volume for each treatment group.

clearly indicate endothelial cell effects of vandetanib and docetaxel treatments, the docetaxel dose and frequency did not appear to have different effects on tumor endothelium but did appear to affect overall tumor growth characteristics.

Discussion

Preclinical pharmacokinetic models capable of predicting concentrations/exposure *in vivo* under different dosing schema can provide an invaluable tool for the rational design of clinical dosing protocols. The overall goals of the

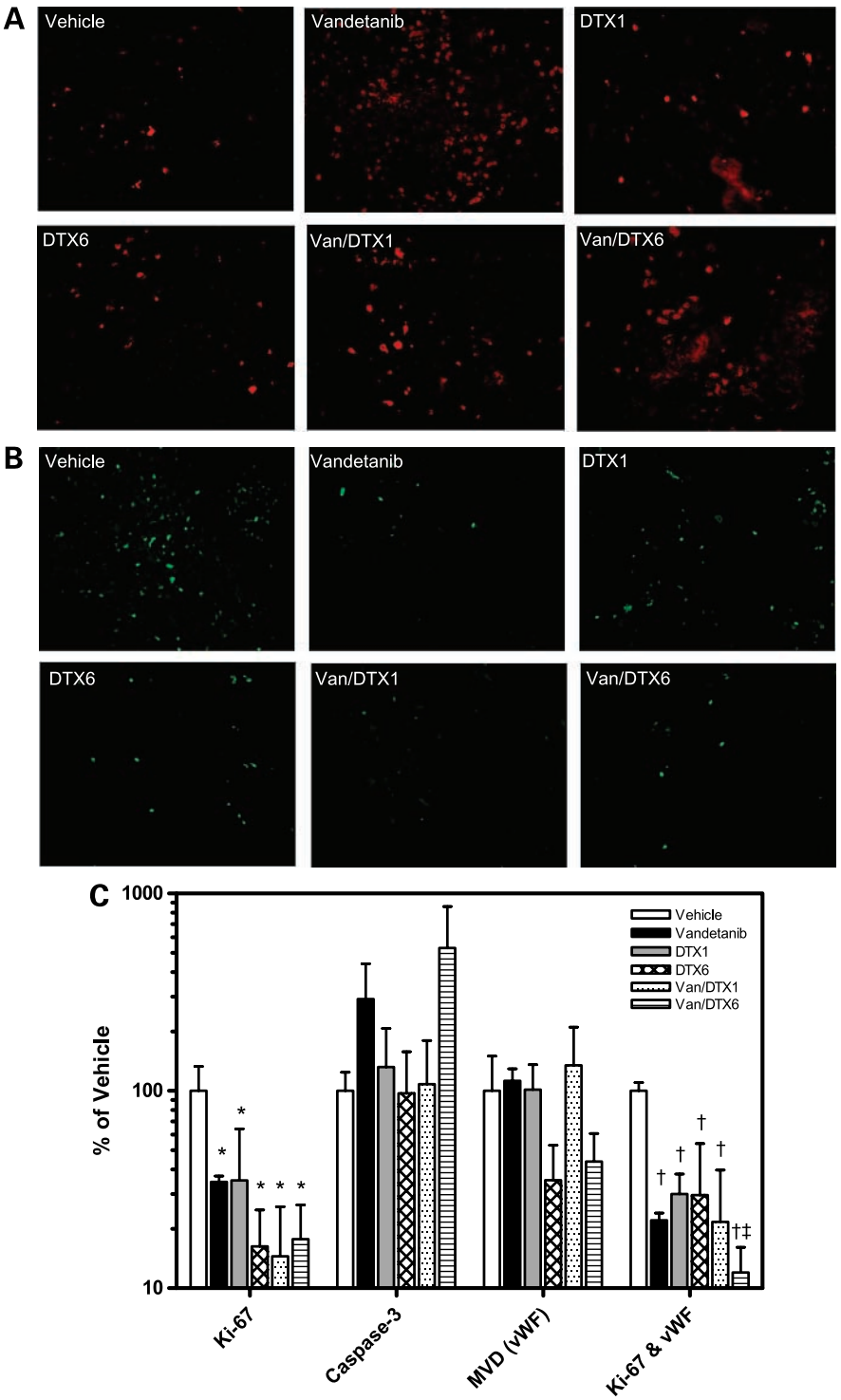

Figure 5. Immunohistochemical analysis of apoptosis (**A**) and proliferation (**B**) in UMSCC2 tumor sections from mice treated with vandetanib, docetaxel, and combination of the two. Three animals per group were sacrificed on day 10 of treatment, approximately 2 h post-treatment, and tumors were removed and formalin fixed. Activated caspase-3, used to determine apoptosis, was visualized by an active caspase-3 rabbit anti-mouse/human antibody followed by Texas red anti-rabbit IgG. Ki-67, used to determine proliferation, was visualized by a rat anti-mouse monoclonal antibody followed by a FITC-conjugated anti-rat IgG. **C,** quantitative analysis of activated caspase-3, Ki-67, vWF, and dual vWF/Ki-67 on UMSCC2 tumor sections. Mean ± SD of data obtained from sections from three different tumors from each treatment group.

studies described herein were to design and evaluate the use of rational dosing protocols for vandetanib, docetaxel, and combinations of the two using pharmacokinetically directed dosing protocols that were reflective of exposures attainable in humans and that target antitumor and antiangiogenic responses. We utilized a PBPK model for docetaxel to develop dosing protocols that would allow us to examine the effects of standard docetaxel treatment versus a metronomic or antiangiogenic schedule of docetaxel. Pharmacokinetic data on vandetanib was used to determine a steady-state dose level that was reflective of human vandetanib exposure (32).

Preclinical testing is an integral part of the development of new therapeutics and new therapeutic strategies. With increasing interest in angiogenesis as a cancer therapy target, either through metronomic scheduling of chemotherapeutics, molecularly targeted agents, or a combinations of the two, the need for appropriate *in vitro* and *in vivo* models is essential. We first established antiproliferative activity of docetaxel, vandetanib, and combinations of the two in murine primary endothelial cells of lung and tumor origin. Murine endothelial cells were selected because the vasculature that supports the growth and maintenance of human tumor cell line xenografts is of murine origin regardless of the tumor type or species of origin (38). Due to the difficulty in isolating pure populations of murine endothelial cells from tumors, and the short duration in which these cells can remain in culture, we wanted to determine if endothelial cells isolated from normal tissue would respond similarly to treatment and therefore serve as a reasonable alternative *in vitro* cell model for future experiments. We also determined the antiproliferative effects of vandetanib and docetaxel in a HNSCC cell line, UMSCC2. These data were used to establish desired *in vivo* plasma concentrations to target to achieve an antiendothelial effect.

Our results showed that primary endothelial cells derived from mouse lung and from tumor xenografts respond similarly to vandetanib, docetaxel, and combination of the two *in vitro* and that vandetanib additively to synergistically enhanced docetaxel growth inhibition. Both cell lines were relatively sensitive to docetaxel treatment with median lethal dose values in the low nanomolar range. Based on these data and on data from previously published studies examining endothelial cell treatment with docetaxel (26), we decided to develop an antiangiogenic dose schedule with the use of our route-modified PBPK model that maintained a minimum plasma concentration of 1 nmol/L for the course of the study.

Unexpectedly, the low-dose metronomic schedule of 1 mg/kg/d docetaxel resulted in severe toxicity and significant death (17 of 18 animals). Ten days into the daily treatment schedule, we modified the schedule to include a 9-day break period. Because the daily dose of docetaxel administered was significantly lower than MTD doses (~20 mg/kg; ref. 39) and even our own 6 mg/kg dose, we speculate that the frequency of treatment may have resulted in a sort of continuous reservoir of docetaxel in the peritoneal cavity, which resulted in the dramatic and severe intestinal toxicity observed. Only mild toxicity was observed in animals treated with 6 mg/kg docetaxel with some, but significantly less, death than the 1 mg/kg groups (3 of 17 animals).

Our pharmacokinetic-directed dose schedules for docetaxel and vandetanib were tested in a mouse xenograft model of HNSCC to determine antitumor and antiendothelial responses. Tumor growth inhibition data showed that all treatment groups had some effect on reducing tumor growth with the greatest effect in groups given vandetanib with docetaxel. Despite the significant effect of the various treatment regimens, it is important to note that tumor regression was not observed in the majority of animals; merely a reduction in tumor growth versus control was observed. Additionally, once treatment was discontinued, the tumors that remained began to regrow in all treatment groups in surviving animals. The immunohistochemical analysis of tumors on day 10 of treatment revealed significant effects of treatment only on total (tumor and endothelium) proliferation and endothelial cell proliferation as measured by Ki-67 and Ki-67/vWF dual staining of tumor sections. Although trends in caspase-3 staining and microvessel density were observed, these results were not significant. Immunohistochemical results are relatively consistent with tumor growth data, indicating that in general vandetanib added to docetaxel therapy resulted in the most dramatic antitumor and antiendothelial effects. Although it is difficult to clearly ascertain, due to the severe toxicity and death observed, it appears that the metronomic dosing protocol developed for docetaxel was not as effective as higher dose docetaxel or even single-agent vandetanib treatment in this tumor model.

The majority of published preclinical studies that have demonstrated single-agent efficacy of vandetanib have used doses (25-100 mg/kg; refs. 12, 13, 40), which would not be reflective of exposures attainable in humans. Our study used a dose that was reflective of exposures measured in humans at 100 to 300 mg/d (32, 41). Additionally, our selected dose of 15 mg/kg/d achieved steady-state plasma minimum and maximum plasma concentrations (C_{min} and C_{max}, approximately 1.4 and 3.3 μmol/L, respectively; ref. 32) in mice capable of inhibiting tumor and endothelial cell growth *in vitro* and *in vivo*.

The use of vandetanib in the clinic will probably involve combinations with other treatment modalities. Our *in vitro* and *in vivo* study findings are in agreement with several preclinical and clinical studies that have indicated that molecularly target agents, such as vandetanib, provide added benefit to chemotherapy (13, 16, 42, 43). Our growth inhibition studies in primary endothelial cells showed that subtoxic levels of vandetanib (1 μmol/L) significantly enhanced the effects of docetaxel treatment in endothelial cells. Numerous studies have shown that cytotoxic chemotherapy on endothelial cells can be diminished by the presence of growth factors such as basic fibroblast growth factor or VEGF (26, 44, 45). As a result, the addition of vandetanib may enhance the growth inhibitory effects of

docetaxel by blocking the prosurvival pathways activated by growth factors.

The use of pharmacokinetic and PBPK models to design dosing protocols to be tested preclinically is the most rational approach to developing cancer therapies that will be clinically effective. Often, doses of drugs used in preclinical models far exceed what is attainable in humans. The use of dose levels that are reflective of exposures measured or estimated in human populations may serve to improve the ability of preclinical models to better predict therapies and schedules that will be effective in obtaining tumor response clinically. Although we were unable to clearly test metronomic versus MTD schedules of docetaxel alone and in combination with vandetanib in these studies, due to toxicity observed with metronomic schedules through i.p. administration, we were able to use a PBPK model and pharmacokinetic data to develop dosing regimens to effectively treat HNSCC cell xenografts at concentrations relevant to exposures in humans. Since repeated, frequent i.p. administration of docetaxel is not a reasonable approach for the evaluation of MTD versus metronomic schedules, we feel it is worth investigating other routes of administration.

Disclosure of Potential Conflicts of Interest

No potential conflicts of interest were disclosed.

Acknowledgments

We thank AstraZeneca for generous gift of vandetanib, Sanofi-Aventis for generous gift of docetaxel, Dr. Barbara Frederick for providing cells and for helpful discussions, Andrea Merz for assistance with the animal treatments, and Dr. E.J. Ehrhart for assistance with the immunohistochemistry.

References

1. Folkman J. Tumor angiogenesis: therapeutic implications. N Engl J Med 1971;285:1182 – 6.

2. Ferrara N. Vascular endothelial growth factor. Eur J Cancer 1996;32A: 2413 – 22.

3. Jain R. Molecular recognition of vessel maturation. Nat Med 2003;9: 685 – 93.

4. Ferrara N. Vascular endothelial growth factor as a target for anticancer therapy. Oncologist 2004;9:2 – 10.

5. Nicholson RI, Gee JMW, Harper ME. EGFR and cancer prognosis. Eur J Cancer 2001;37:S9 – 15.

6. Baker CH, Kedar D, McCarty MF, et al. Blockade of epidermal growth factor receptor signaling on tumor cells and tumor-associated endothelial cells for therapy of human carcinomas. Am J Pathol 2002;161:929 – 38.

7. Sasaki T, Kitadai Y, Nakamura T, et al. Inhibition of epidermal growth factor receptor and vascular endothelial growth factor receptor phosphorylation on tumor-associated endothelial cells leads to treatment of orthotopic human colon cancer in nude mice. Neoplasia 2007;9:1066 – 77.

8. Hynes N, Lane H. ErbB receptors and cancer: the complexity of targeted inhibitors. Nat Rev Cancer 2005;5:580.

9. Rogers S, Harrington K, Rhys-Evans P, O-Charoenrat P, Eccles S. Biological significance of c-ErbB family oncogenes in head and neck cancer. Cancer Metastasis Rev 2005;24:47 – 69.

10. Hennequin LF, Stokes ESE, Thomas AP, et al. Novel 4-anilinoquinazolines with C-7 basic side chains: design and structure activity relationship of a series of potent, orally active, VEGF receptor tyrosine kinase inhibitors. J Med Chem 2002;45:1300 – 12.

11. Hennequin LF, Thomas AP, Johnstone C, et al. Design and structure-activity relationship of a new class of potent VEGF receptor tyrosine kinase inhibitors. J Med Chem 1999;42:5369 – 89.

12. Wedge SR, Ogilvie DJ, Dukes M, et al. ZD6474 inhibits vascular endothelial growth factor signaling, angiogenesis, and tumor growth following oral administration. Cancer Res 2002;62:4646 – 55.

13. Ciardiello F, Caputo R, Damianco V, et al. Antitumor effects of ZD6474, a small molecule vascular endothelial growth factor receptor tyrosine kinase inhibitor, with additional activity against epidermal growth factor receptor tyrosine kinase. Clin Cancer Res 2003;9:1546 – 56.

14. Williams K, Telfer B, Brave S, et al. ZD6474, a potent inhibitor of vascular endothelial growth factor signaling, combined with radiotherapy: schedule-dependent enhancement of antitumor activity. Clin Cancer Res 2004;10:8587 – 93.

15. Damianco V, Melisi D, Bianco C, et al. Cooperative antitumor effect of multitargeted kinase inhibitor ZD6474 and ionizing radiation in glioblastoma. Clin Cancer Res 2005;11:5639 – 44.

16. Heymach JV, Johnson BE, Prager D, et al. Randomized, placebo-controlled phase II study of vandetanib plus docetaxel in previously treated non-small cell lung cancer. J Clin Oncol 2007;25:4270 – 7.

17. Gueritte-Voegelein F, Guenard D, Lavelle F, et al. Relationships between the structure of Taxol analogues and their antimitotic activity. J Med Chem 1991;34:992 – 8.

18. Engels F, Verweij J. Docetaxel administration schedule: from fever to tears? A review of randomised studies. Eur J Cancer 2005;41:1117 – 26.

19. Lyseng-Williamson K, Fenton C. Docetaxel: a review of its uses in metastatic breast cancer. Drugs 2005;65:2513 – 31.

20. Belani C. Optimizing chemotherapy for advanced non-small cell lung cancer: focus on docetaxel. Lung Cancer 2005;50:S3 – 8.

21. Engels F, Sparreboom A, Mathot R, Verweij J. Potential for improvement of docetaxel-based chemotherapy: a pharmacological review. Br J Cancer 2005;93:173 – 7.

22. Suzuki M, Nishimura Y, Nakamatsu K, et al. Phase I study of weekly docetaxel infusion and concurrent radiation therapy for head and neck cancer. Jpn J Clin Oncol 2003;33:297 – 301.

23. Allal AS, Zwahlen D, Becker M, Dulguerov P, Mach N. Phase I trial of concomitant hyperfractionated radiotherapy with docetaxel and cisplatin for locally advanced head and neck cancer. Cancer J 2006;12:63 – 8.

24. Kalyankrishna S, Grandis J. Epidermal growth factor receptor biology in head and neck cancer. J Clin Oncol 2006;24:2666 – 72.

25. Bonner B, Harari P, Giralt J, et al. Radiotherapy plus cetuximab for squamous cell carcinoma of the head and neck. N Engl J Med 2006;354: 567 – 78.

26. Sweeny CJ, Miller KD, Sissons SE, et al. The antiangiogenic property of docetaxel is synergistic with a recombinant humanized monoclonal antibody against vascular endothelial growth factor or 2-methoxyestradiol but antagonized by endothelial growth factors. Cancer Res 2001;61:3369 – 72.

27. Grant D, Williams T, Zahaczewsky M, Dicker A. Comparison of antiangiogenic activities using paclitaxel (Taxol) and docetaxel (Taxotere). Int J Cancer 2003;104:121 – 9.

28. Hotchkiss K, Ashton A, Mahmood R, et al. Inhibition of endothelial cell function *in vitro* and angiogenesis *in vivo* by docetaxel (Taxotere): association with impaired repositioning of the microtubule organizing center. Mol Cancer Ther 2002;1:1191 – 200.

29. Baker S, Zhao M, Lee C, et al. Comparative pharmacokinetics of weekly and every-three-weeks docetaxel. Clin Cancer Res 2006;10:1976 – 83.

30. Chen H-SG, Gross J. Physiologically based pharmacokinetic models for anticancer drugs. Cancer Chemother Pharmacol 1979;2:85 – 94.

31. Bradshaw-Pierce EL, Eckhardt SG, Gustafson DL. A physiologically based pharmacokinetic model of docetaxel disposition: from mouse to man. Clin Cancer Res 2007;13:2768 – 76.

32. Gustafson DL, Bradshaw-Pierce EL, Merz AL, Zirrolli JA. Tissue distribution and metabolism of the tyrosine kinase inhibitor ZD6474 (Zactima) in tumor-bearing nude mice following oral dosing. J Pharmacol Exp Ther 2006;318:872 – 80.

33. Marelli-Berg FM, Peek E, Lidington EA, Stauss HJ, Lechler RI. Isolation of endothelial cells from murine tissue. J Immunol Methods 2000;244:205 – 15.

34. St.Croix B, Rago C, Velculescu V, et al. Genes expressed in human and tumor endothelium. Science 2000;289:1197 – 202.

35. Sartorius C, Shen T, Horwitz K. Progesterone receptors A and B differentially affect the growth of estrogen-dependent human breast tumor xenografts. Breast Cancer Res Treat 2003;79:287 – 99.

36. Chou T-C. Relationships between inhibition constants and fractional inhibitions in enzyme-catalyzed reactions with different numbers of

reactants, different reaction mechanisms, and different types of mechanisms of inhibition. Mol Pharm 1974;10:235 – 47.

37. Chou T-C. Derivation and properties of Michaelis-Menton type and Hill type equations for reference ligands. J Theor Biol 1976;39:253 – 76.

38. Walter-Yohrling J, Morgenbesser S, Rouleau C, et al. Murine endothelial cell lines as a model of tumor endothelial cells. Clin Cancer Res 2004;10:2179 – 89.

39. Dykes D, Bissery M, Harrison SJ, Waud W. Response of human tumor xenografts in athymic nude mice to docetaxel (RP 56976, Taxotere). Invest New Drugs 1995;13:1 – 11.

40. Ciardiello F, Bianco R, Caputo R, et al. Antitumor activity of ZD6474, a vascular endothelial growth factor receptor tyrosine kinase inhibitor, in human cancer cells with acquired resistance to antiepidermal growth factor receptor activity. Clin Cancer Res 2004;10:784 – 93.

41. Holden S, Eckhardt S, Basser R, et al. Clinical evaluation of ZD6474, an orally active inhibitor of VEGF and EGF receptor signaling, in patients with solid, malignant tumors. Ann Oncol 2005;16:1391 – 7.

42. Bianco C, Giovannetti E, Ciardiello F, et al. Synergistic antitumor activity of ZD6474, an inhibitor of vascular endothelial growth factor receptor and epidermal growth factor receptor signaling, with gemcitabine and ionizing radiation against pancreatic cancer. Clin Cancer Res 2006;12: 7099 – 107.

43. Troiani T, Serkova NJ, Gustafson DL, et al. Investigation of two dosing schedules of vandetanib (ZD6474), an inhibitor of vascular endothelial growth factor receptor and epidermal growth factor receptor signaling, in combination with irinotecan in a human colon cancer xenograft model. Clin Cancer Res 2007;13:6450 – 8.

44. Tran J, Master Z, Yu JL, Rak J, Dumont DJ, Kerbel RS. A role for survivin in chemoresistance of endothelial cells mediated by VEGF. Proc Natl Acad Sci U S A 2002;99:4349 – 54.

45. Gerber H-P, McMurtrey A, Kowalski J, et al. Vascular endothelial growth factor regulates endothelial cell survival through the phosphatidylinositol 3′-kinase/Akt signal transduction pathway. J Biol Chem 1998; 273:30336 – 43.

Molecular Cancer Therapeutics

Pharmacokinetic-directed dosing of vandetanib and docetaxel in a mouse model of human squamous cell carcinoma

Erica L. Bradshaw-Pierce, Courtney A. Steinhauer, David Raben, et al.

Mol Cancer Ther 2008;7:3006-3017.